Heavy quasiparticles and Cooper-pair interaction in the Hubbard model

Fusayoshi J. Ohkawa
Department of Physics, Hokkaido University, Sapporo 060, Japan
(Received 4 October 1994; revised manuscript received 28 May 1996)

The Hubbard model is studied in the vicinity of the Mott transition. Local and quantal spin fluctuations are completely included through the mapping to the Anderson model; a local Kondo temperature T_K is defined as their characteristic temperature or energy scale. Antiferromagnetic spin fluctuations are included perturbatively in terms of $1/d$ and to leading order in $k_B T_K/U$ with d being the spatial dimensionality, k_B the Boltzmann constant, and U the intrasite repulsion. The two different kinds of spin fluctuations are responsible for the formation of heavy quasiparticles. Two intersite exchange interactions are responsible for both the development of the antiferromagnetic spin fluctuations and $d\gamma$-wave Cooper pairing between the heavy quasiparticles: the superexchange interaction and an exchange interaction due to the virtual exchange of spin excitations within the heavy quasiparticle band. An experimental specific-heat coefficient of about 14 $\mathrm{mJ/K^2\ CuO_2}$ mol and a Wilson ratio of about 0.4 imply that the interplay between the local and the antiferromagnetic spin fluctuations plays a crucial role in both the normal and the superconducting states of $\mathrm{YBa_2Cu_3O_{7-\delta}}$ with critical temperatures of $T_c \simeq 90$ K. A pairing interaction deduced from the normal-state properties is strong enough to give critical temperatures as high as $T_{c0} \simeq 200$ K in the absence of any pair breaking; there is experimental evidence that the pair-breaking effect of the antiferromagnetic spin fluctuations reduces $T_{c0} \simeq 200$ K down to $T_c \simeq 90$ K. [S0163-1829(96)05845-6]

I. INTRODUCTION

It is of great importance to elucidate the mechanism of high-temperature (high-T_c) superconductivity of cuprate oxides.[1] It occurs in the vicinity of the Mott transition or instability of local-moment antiferromagnetism. Electrons that are almost localized because of strong correlations must play a leading role in the high-T_c superconductivity. Then the question arises of whether or not the *normal* state of cuprate oxides is Landau's normal Fermi liquid.[2] We assume in this paper that it is the normal Fermi liquid.[3]

Another question is, what is a dominant pairing interaction in cuprate oxides? In general, charge fluctuations are substantially depressed in strongly correlated electron liquids. The virtual exchange of charge excitations is unlikely to cause a strong pairing interaction.

Any phonon mechanism is not promising either. An experimental specific-heat coefficient[4] of $\gamma \simeq 14$ $\mathrm{mJ/K^2\ CuO_2}$ mol tells that the effective mass of quasiparticles is about 10 times as large as that according to band calculation: The mass-renormalization factor ϕ_m of quasiparticles is about 10. An electron-phonon interaction is unlikely to cause such a large mass renormalization; a possible scenario describes that the large mass renormalization is due to the strong correlations between electrons, while the virtual exchange of phonons is responsible for Cooper pairing. However, this scenario is difficult to accept; vertex renormalizations are unlikely to compete with a large mass renormalization. Two kinds of vertex corrections have to be considered: the vertex correction due to an electron-phonon interaction and the vertex correction due to the strong correlations. The former is so small as to be ignored.[5] The latter is nothing but the vertex correction for the charge channel, that for an interaction due to the virtual exchange of charge excitations. Because charge fluctuations are depressed, the vertex function φ_c for the charge channel is also depressed: $\varphi_c < 1$. What plays a crucial role in this scenario is not a bare pairing interaction I_{ph}, itself, but $I_{\mathrm{ph}}(\varphi_c/\phi_m)^2$. It is unlikely that $I_{\mathrm{ph}}(\varphi_c/\phi_m)^2$ is large enough to reproduce observed critical temperatures of $T_c \simeq 100$ K.

On the other hand, a magnetic mechanism is promising. The high-T_c superconductivity occurs essentially in the $\mathrm{CuO_2}$ planes. On the basis of an idea[6] that the superexchange interaction can be a Cooper-pairing interaction, it has been argued[7] that one of the simplest effective Hamiltonians for cuprate oxides is the Hubbard model on the simple square lattice in the large-U regime defined by $U/|t| > 8$ or $U/|t| \gg 1$, with U being the intrasite repulsion and t the transfer integral between the nearest neighbors. The gap equation for $d\gamma$-wave Cooper pairing has been solved in a previous paper;[8] within the theoretical framework of the normal Fermi liquid, the superexchange interaction between the nearest neighbors, and an intrasite effective strong repulsion,[9] critical temperatures of the $d\gamma$-wave Cooper pairing are substantially higher than those of other types of Cooper pairing.[10] Actually, many experiments imply that the $d\gamma$-wave Cooper pairing occurs in cuprate oxides: the absence of the Hebel-Slichter peak in the nuclear magnetic relaxation (NMR) rate,[11–14] the temperature-linear penetration depth,[15] the angle-resolved photoemission spectra,[16] and the π shift in the Josephson interference experiment.[17,18]

The previous paper[8] contains two crucial parameters: the bandwidth of quasiparticles and an effective pairing interaction $J_1(\varphi_s/\phi_m)^2$, with J_1 being the nearest-neighbor component of the exchange interaction and φ_s the vertex function for the spin channel. The bandwidth is assumed to be 0.4 eV; it is almost the same as the value deduced from the experimental $\gamma \simeq 14$ $\mathrm{mJ/K^2\ CuO_2}$ mol.[4] From the physical properties of insulating phases, J_1 is estimated to be 0.10–0.15

eV.[19,20] In a single-site approximation (SSA) that has been developed for Kondo lattices or the so-called heavy-electron liquids φ_s/ϕ_m is nothing but the Wilson ratio for the Kondo problem. When charge fluctuations are depressed, $\varphi_s/\phi_m \simeq 2$.[21–24] We then obtain $J_1(\varphi_s/\phi_m)^2 = 0.40-0.60$ eV. However, according to Fig. 2 of Ref. 8, this value is too large to reproduce the observed $T_c \simeq 100$ K. This drawback implies that the normal state has to be studied in an approximation beyond the SSA.

Two theories for the Hubbard model, proposed in 1963, are distinguished in a study of strongly correlated electron liquids.[25–27] According to one of these theories, the Gutzwiller heavy quasiparticle band is present at the chemical potential for almost half filling.[25] According to another theory, the band splits into the lower and upper Hubbard bands.[26] Although they apparently contradict each other, both of them are physically reasonable: It has recently been demonstrated that the Gutzwiller band lies between the lower and upper Hubbard bands.[28] The two different theories are concerned with different energy states: the ground state and the excited states.

Much progress has recently been achieved in the study of strongly correlated electron liquids. The SSA that considers all the single-site terms is rigorous in the large limit of the coordination number of lattices[29] or the spatial dimensionality d.[30] Solving the Hubbard model in the SSA is reduced to solving the Anderson model.[31–33] The Anderson model as well as the s-d model is an effective Hamiltonian for the Kondo problem or the Kondo effect. The appearance of magnetic moments is quenched by the Kondo effect in strongly correlated electron liquids as well as in dilute magnetic alloys. In other words, local and quantal spin fluctuations are responsible for the quenching of the magnetic moments and for the formation of the Gutzwiller heavy quasiparticle band. Thus the Gutzwiller band is nothing but the Abrikosov-Suhl or the Kondo resonance peak; its effective bandwidth corresponds to the so-called Kondo temperature.

The superexchange interaction is present even in metallic phases;[34] the band splitting into the lower and upper Hubbard bands occurs similarly in both insulating and metallic phases, and it is due to the virtual exchange of spin excitations between them. Its nearest-neighbor component is of the order of $t^2/(dU)$ or $O(1/d)$. The multisite terms[35] that are ignored in the SSA can be considered by the $1/d$ expansion method.[32,33] For example, consider Weiss's magnetic mean fields. Because the number of the nearest neighbors is of the order of d, the mean fields are of leading order in $1/d$ or $O(1)$; the magnetic instability is $O(1)$. The quenching of the magnetic moments by the local and quantal spin fluctuations is also $O(1)$. Whether the ground state is magnetic or paramagnetic is determined by the competition between the two leading-order effects in $1/d$.

One of the most essential and difficult problems in the study of strong correlated electron liquids is to treat the local and quantal spin fluctuations; one of the greatest advantages of the $1/d$ expansion method is that many established results for the Kondo effect are available for this treatment. The Kondo problem has already been settled;[21] the Kondo effect is well understood now;[22–24,36] even an exact solution has been obtained by the Bethe method.[37–39] As is argued in Appendix A the starting or unperturbed state of the $1/d$ expansion method is definitely the normal Fermi liquid. The $1/d$ expansion method is physically a perturbative method of treating intersite effects by starting from the Fermi liquid. Another advantage is that it is a perturbative scheme, in essence, in terms of $t^2/(dU)$ instead of U; it is easy to treat intersite effects in the large U regime.

The competition among antiferromagnetism, superconductivity, and other kinds of instabilities has already been studied by treating the superexchange interaction perturbatively in a previous paper;[10] it is nothing but a treatment by the $1/d$ expansion method. A recent study[40] by the $1/d$ expansion method has confirmed a phase diagram of Ref. 10: The ground state is antiferromagnetic for almost half filling, and is the condensed state of $d\gamma$-wave Cooper pairs between heavy quasiparticles a little bit away from half filling. This recent study[40] implies that the low dimensionality of cuprate oxides must be crucial for the high-T_c superconductivity; anisotropic superconductivity is of higher order in $1/d$.

However, the normal state has been considered to leading order in $1/d$ in Ref. 40. One of the purposes of this paper is to study two types of renormalizations: the mass renormalization of quasiparticles due to two different kinds of spin fluctuations, the local and quantal spin fluctuations and intersite spin fluctuations, and vertex renormalizations due to them; the two types of renormalizations due to the intersite spin fluctuations are of higher order in $1/d$. Another purpose is to show that a magnetic pairing interaction is present in addition to the superexchange interaction; it is also shown that when the intersite spin fluctuations are developed the magnetic pairing interactions are enhanced. The other purpose is to apply theoretical results on these issues to cuprate oxides to explain the critical temperatures of $T_c \simeq 100$ K.

The plan of this paper is as follows. In Sec. II, a Fermi-liquid theory is developed by using the $1/d$ expansion method; the two types of renormalizations are considered. The magnetic pairing interactions and their enhancement are considered in Sec. III. The specific heat from the intersite spin fluctuations is considered in Sec. IV. In Sec. V, we apply results of Secs. II, III, and IV to cuprate-oxide superconductors. A discussion is given in Sec. VI, and a conclusion in Sec. VII. It is shown in Appendix A that the unperturbed state of the $1/d$ expansion method is the normal Fermi liquid. An argument on the Mott transition is given in Appendix B.

II. FERMI-LIQUID THEORY

It is shown in this section that there is another small expansion parameter in addition to $1/d$; the normal state can be described by only few Fermi-liquid parameters because of these two small parameters.

Consider the Hubbard model on the simple hypercubic lattice in d dimensions:

$$\mathcal{H} = -t\sqrt{\frac{2}{d}}\sum_{\langle ij\rangle\sigma} a_{i\sigma}^{\dagger}a_{j\sigma} + \frac{1}{2}U\sum_{i\sigma} a_{i\sigma}^{\dagger}a_{i\sigma}a_{i-\sigma}^{\dagger}a_{i-\sigma}, \qquad (2.1)$$

with $\langle ij\rangle$ standing for the nearest neighbors. The dispersion relation of unrenormalized electrons measured from the chemical potential μ is given by

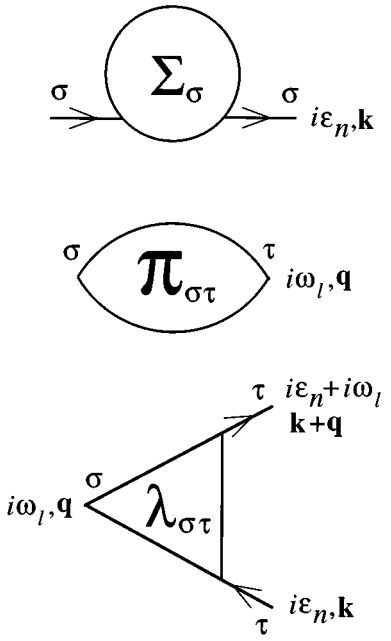

FIG. 1. Arguments of the self-energy, the polarization, and the three-point vertex functions.

$$E(\mathbf{k}) = -2t\sqrt{\frac{2}{d}}\sum_{\nu=1}^{d}\cos(k_\nu a) - \mu, \tag{2.2}$$

with k_ν being the νth component of wave-number vector $\mathbf{k}$ and a the lattice constant. An effective bandwidth is $O(|t|)$ for any d.[30] We are mainly interested in the Hubbard model on the simple square lattice ($d=2$).

Consider the self-energy function $\Sigma_\sigma(i\varepsilon_n,\mathbf{k})$, the polarization function $\pi_{\sigma\tau}(i\omega_\ell,\mathbf{q})$, and the three-point vertex function $\lambda_{\sigma\tau}(i\varepsilon_n, i\varepsilon_n+i\omega_\ell;\mathbf{k},\mathbf{k}+\mathbf{q})$, which are irreducible. Here $\varepsilon_n=(2n+1)\pi k_B T$ and $\omega_\ell=2\ell\pi k_B T$ with n being an integer, ℓ another integer, k_B the Boltzmann constant, and T temperature. Figure 1 shows definitions of their arguments of spins, energies, and momenta. Any diagram for the irreducible self-energy can never be divided into two parts by cutting a single electron line; any diagram for the polarization and the vertex functions that are irreducible can never be divided into two parts by removing a single U line. The polarization and the vertex functions for the charge and the longitudinal spin channels are then given by

$$\pi_c(i\omega_\ell,\mathbf{q}) = \pi_{\sigma\sigma}(i\omega_\ell,\mathbf{q}) + \pi_{\sigma-\sigma}(i\omega_\ell,\mathbf{q}), \tag{2.3}$$

$$\pi_s(i\omega_\ell,\mathbf{q}) = \pi_{\sigma\sigma}(i\omega_\ell,\mathbf{q}) - \pi_{\sigma-\sigma}(i\omega_\ell,\mathbf{q}), \tag{2.4}$$

$$\begin{aligned}\lambda_c(i\varepsilon_n, i\varepsilon_n+i\omega_\ell;\mathbf{k},\mathbf{k}+\mathbf{q}) &= \lambda_{\sigma\sigma}(i\varepsilon_n, i\varepsilon_n+i\omega_\ell;\mathbf{k},\mathbf{k}+\mathbf{q}) \\ &\quad + \lambda_{\sigma-\sigma}(i\varepsilon_n, i\varepsilon_n+i\omega_\ell;\mathbf{k},\mathbf{k}+\mathbf{q}),\end{aligned} \tag{2.5}$$

and

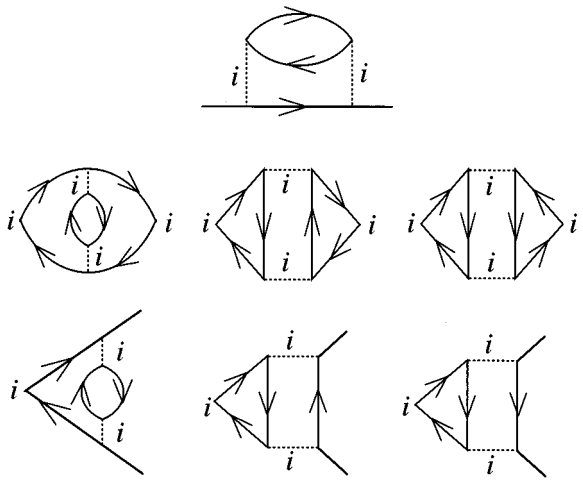

FIG. 2. Single-site diagrams for the self-energy, the polarization, and the vertex functions, whose skeleton diagrams are of second order in U. Single-site indices appear in the diagrams. A solid line stands for the renormalized single-particle Green function that is site diagonal, and a dotted line for U.

$$\begin{aligned}\lambda_s(i\varepsilon_n, i\varepsilon_n+i\omega_\ell;\mathbf{k},\mathbf{k}+\mathbf{q}) &= \lambda_{\sigma\sigma}(i\varepsilon_n, i\varepsilon_n+i\omega_\ell;\mathbf{k},\mathbf{k}+\mathbf{q}) \\ &\quad - \lambda_{\sigma-\sigma}(i\varepsilon_n, i\varepsilon_n+i\omega_\ell;\mathbf{k},\mathbf{k}+\mathbf{q})\end{aligned} \tag{2.6}$$

respectively.

In a next step their skeleton diagrams are written down by treating U perturbatively in the site representation. When single-site indices appear in the diagrams, they are called single-site diagrams. Examples of the single-site diagrams are shown in Fig. 2. All the other diagrams are called multisite diagrams.[35] The electron lines are then replaced by renormalized lines, which stand for

$$R_{ij\sigma}(i\varepsilon_n) = \frac{1}{N}\sum_{\mathbf{k}} e^{i\mathbf{k}\cdot(\mathbf{R}_i-\mathbf{R}_j)} G_\sigma(i\varepsilon_n,\mathbf{k}), \tag{2.7}$$

with

$$G_\sigma(i\varepsilon_n,\mathbf{k}) = \frac{1}{i\varepsilon_n - E(\mathbf{k}) - \Sigma_\sigma(i\varepsilon_n,\mathbf{k})}, \tag{2.8}$$

and all the diagrams are summed up. They are divided into the single-site and the multisite terms; we find, for example,

$$\Sigma_\sigma(i\varepsilon_n,\mathbf{k}) = \tilde{\Sigma}_\sigma(i\varepsilon_n) + \Delta\Sigma_\sigma(i\varepsilon_n,\mathbf{k}), \tag{2.9}$$

$$\pi_s(i\omega_\ell,\mathbf{q}) = \tilde{\pi}_s(i\omega_\ell) + \Delta\pi_s(i\omega_\ell,\mathbf{q}), \tag{2.10}$$

and

$$\begin{aligned}\lambda_s(i\varepsilon_n, i\varepsilon_n+i\omega_\ell;\mathbf{k},\mathbf{k}+\mathbf{q}) &= \tilde{\lambda}_s(i\varepsilon_n, i\varepsilon_n+i\omega_\ell) + \Delta\lambda_s(i\varepsilon_n, i\varepsilon_n+i\omega_\ell;\mathbf{k},\mathbf{k}+\mathbf{q})\end{aligned} \tag{2.11}$$

in the wave-number representation, where the first and the second terms on the right side are the single-site and the

multisite terms, respectively. The single-site terms are of leading order in $1/d$. The multisite terms are of higher order in $1/d$ except for specific $\mathbf{q}$'s.

The single-site terms are given by the solutions of a mapped Anderson model (MAM), when

$$R_{ii\sigma}(i\varepsilon_n)=\widetilde{G}_{dd\sigma}(i\varepsilon_n) \tag{2.12}$$

is satisfied[31,41] with $\widetilde{G}_{dd\sigma}(i\varepsilon_n)$ being the renormalized Green function for strongly correlated electrons of the MAM. The mapping condition of Eq. (2.12) is nothing but the self-consistency condition to solve the MAM. This is the renormalized single-site approximation (RSSA).[41] The multisite self-energy appears in the mapping condition through Eq. (2.8); the RSSA depends on the multisite self-energy. Although we had better call the single-site terms in the RSSA renormalized single-site terms, we call them simply the single-site terms in this paper. The RSSA is rigorous for the Fermi liquid[42] if no approximation is made for the multisite self-energy. Even if the multisite self-energy is ignored, it is rigorous for the Fermi liquid in infinite dimensions.

We find from Eq. (2.12) that the density of states of the Hubbard model is the same as that of the Anderson model:

$$\rho(\varepsilon)=-\frac{1}{\pi}\mathrm{Im}R_{ii\sigma}(\varepsilon+i0)=-\frac{1}{\pi}\mathrm{Im}\widetilde{G}_{dd\sigma}(\varepsilon+i0). \tag{2.13}$$

It has the three-peak structure in the large-U regime and for almost half filling as is discussed in the Introduction. Recent numerical studies[43–46] have demonstrated the existence of the three-peak structure in infinite dimensions.

The susceptibility of the Hubbard model is given by

$$\begin{aligned}\chi_s(i\omega_\nu,\mathbf{q})&\equiv\frac{1}{N}\sum_{j\sigma\sigma'}e^{i\mathbf{q}\cdot(\mathbf{R}_i-\mathbf{R}_j)}\int_0^{1/k_BT}d\tau e^{i\omega_\nu\tau}\sigma\sigma'\\&\quad\times\langle T_\tau a_{i\sigma}^\dagger(\tau)a_{i\sigma}(\tau)a_{j\sigma'}^\dagger a_{j\sigma'}\rangle\\&=\frac{2\pi_s(i\omega_\nu,\mathbf{q})}{1-U\pi_s(i\omega_\nu,\mathbf{q})},\end{aligned} \tag{2.14}$$

where T_τ is the chronological ordering operator, and both of $a_{i\sigma}^\dagger(\tau)$ and $a_{i\sigma}(\tau)$ are the operators in the Heisenberg representation. Consider the MAM in the absence of magnetic fields, and then place only strongly correlated electrons in the presence of magnetic fields. The susceptibility of such an Anderson model is similarly given by

$$\widetilde{\chi}_s(i\omega_\nu)=\frac{2\widetilde{\pi}_s(i\omega_\nu)}{1-U\widetilde{\pi}_s(i\omega_\nu)}, \tag{2.15}$$

where only the polarization of strongly correlated electrons is considered. A local Kondo temperature T_K is defined by

$$[\widetilde{\chi}_s(0)]_{T=0\ \mathrm{K}}=\frac{1}{k_BT_K} \tag{2.16}$$

as a temperature or energy scale of the local and quantal spin fluctuations in the Hubbard model. In the large-U regime, $U\widetilde{\chi}_s(0)\gg1$ and $U\chi_s(0,\mathbf{q})\gg1$; we find from Eqs. (2.14) and (2.15)

$$\pi_s(i\omega_\nu,\mathbf{q})=(1/U)[1+O(1/U\chi_s(0,\mathbf{q}))] \tag{2.17}$$

and

$$\widetilde{\pi}_s(i\omega_\nu)=(1/U)[1+O(1/U\widetilde{\chi}_s(0))] \tag{2.18}$$

for $k_BT\ll U$ and $|\omega_\nu|\ll U$. Considering that $\chi_s(0,\mathbf{q})$ is not much smaller than $\widetilde{\chi}_s(0)$, we find

$$\Delta\pi_s(i\omega_\nu,\mathbf{q})=(1/U)\times O(k_BT_K/U). \tag{2.19}$$

Note that $\Delta\pi_s(i\omega_\nu,\mathbf{q})$ is of higher order not only in $1/d$ but also in $k_BT_K/U\ll1$.

Equation (2.14) gives

$$\chi_s(i\omega_\nu,\mathbf{q})=\left[\frac{1}{\widetilde{\chi}_s(i\omega_\nu)}-\frac{1}{4}I_s(i\omega_\nu,\mathbf{q})\right]^{-1} \tag{2.20}$$

to leading order in k_BT_K/U, with

$$I_s(i\omega_\nu,\mathbf{q})=2U^2\Delta\pi_s(i\omega_\nu,\mathbf{q}). \tag{2.21}$$

Equation (2.21) is an exchange interaction playing a prominent role as is shown in later sections. The static susceptibility is given by

$$\chi_s(\mathbf{q})=\frac{1}{k_BT_K}\frac{1}{1-\alpha(\mathbf{q})}, \tag{2.22}$$

with

$$\alpha(\mathbf{q})=\frac{I_s(0,\mathbf{q})}{4k_BT_K}. \tag{2.23}$$

In this paper, $\chi_s(0,\mathbf{q})$ is simply denoted as $\chi_s(\mathbf{q})$.

We confine our study to $T\ll T_K$; the self-energy of the MAM is expanded in such a way that

$$\widetilde{\Sigma}_\sigma^{(A)}(i\varepsilon_n)=\widetilde{\Sigma}_0+[1-\widetilde{\phi}_m]i\varepsilon_n+[1-\widetilde{\varphi}_s]\sigma H^*+\cdots \tag{2.24}$$

for $|\varepsilon_n|\ll k_BT_K$ in the presence of an infinitesimally small Zeeman energy, $H^*=\frac{1}{2}g\mu_BH$, with g being an effective g factor, μ_B the Bohr magneton, and H a magnetic field. When the energy dependence of the hybridization energy of the MAM can be ignored, we find in general $1\leqslant\widetilde{\varphi}_s/\widetilde{\phi}_m\leqslant2$;[23,24] when charge fluctuations are completely depressed, we find in particular $\widetilde{\varphi}_s/\widetilde{\phi}_m=2$. From this it is likely that $\widetilde{\varphi}_s/\widetilde{\phi}_m\simeq2$ for almost half filling. The self-energy of the Hubbard model is similarly expanded in such a way that

$$\begin{aligned}\Sigma_\sigma(i\varepsilon_n,\mathbf{k})&=\Sigma_0(\mathbf{k})+[1-\phi_m(\mathbf{k})]i\varepsilon_n\\&\quad+[1-\phi_s(\mathbf{k})]\sigma H^*+\cdots,\end{aligned} \tag{2.25}$$

with

$$\Sigma_0(\mathbf{k})=\widetilde{\Sigma}_0+\Delta\Sigma(\mathbf{k}), \tag{2.26}$$

$$\phi_m(\mathbf{k})=\widetilde{\phi}_m+\Delta\phi_m(\mathbf{k}), \tag{2.27}$$

and

$$\phi_s(\mathbf{k})=\widetilde{\phi}_s+\Delta\phi_s(\mathbf{k}), \tag{2.28}$$

where the first and the second terms on the right side of Eqs. (2.26), (2.27), and (2.28) are the single-site and the multisite

terms, respectively. It is trivial that $\tilde{\Sigma}_0$ and $\tilde{\phi}_m$ are the same between the two models but $\tilde{\phi}_s$ is different from $\tilde{\varphi}_s$. The dispersion relation of quasiparticles is given by

$$\xi(\mathbf{k})=[E(\mathbf{k})+\tilde{\Sigma}_0+\Delta\Sigma(\mathbf{k})]/\phi_m(\mathbf{k}), \tag{2.29}$$

and the quasiparticles are heavy for $\phi_m(\mathbf{k})\gg 1$. The coherent part of Eq. (2.8) is described as

$$G_\sigma(i\varepsilon_n,\mathbf{k})=\frac{1}{\phi_m(\mathbf{k})}\,\frac{1}{i\varepsilon_n-\xi(\mathbf{k})}+\cdots. \tag{2.30}$$

It is straightforward to derive expressions for low-temperature properties of the Anderson model[23,24,36] in following Luttinger and Ward.[47,48] The susceptibility in the low-temperature limit is given by

$$\tilde{\chi}_s(0)(1+s_c)=\sum_\sigma\ \tilde{\varphi}_s\left(-\frac{1}{\pi}\right)\mathrm{Im}\tilde{G}_{dd\sigma}(+i0), \tag{2.31}$$

where $\tilde{\chi}_s(0)$ and $\tilde{\chi}_s(0)s_c$ on the left side are due to the polarization of strongly correlated electrons and that of conduction electrons; $\tilde{\chi}_s(0)$ is identical to that given by Eq. (2.16). We assume in this paper that Anderson's compensation theorem[49] is approximately satisfied; $|s_c|\ll 1$. In following Shiba,[36] we find that the inverse of Eq. (2.15) is given by

$$\frac{1}{\tilde{\chi}_s(\omega+i0)}=\frac{1}{\tilde{\chi}_s(0)}-i\,\tfrac{1}{2}\,c_P\pi\omega+\cdots \tag{2.32}$$

for $T\ll T_K$ and $|\omega|\ll k_BT_K$ with

$$c_P=[2\tilde{\varphi}_s\rho(0)/\tilde{\chi}_s(0)]^2=(1+s_c)^2\simeq 1. \tag{2.33}$$

The specific-heat coefficient due to strongly correlated electrons is given by

$$\tilde{\gamma}=\frac{1}{3}\pi^2k_B^2\sum_\sigma\ \tilde{\phi}_m\left(-\frac{1}{\pi}\right)\mathrm{Im}\tilde{G}_{dd\sigma}(+i0)$$

$$=\frac{2\tilde{\phi}_m}{\tilde{\varphi}_s}\,\frac{\pi^2k_B}{6T_K}. \tag{2.34}$$

Those of the Hubbard model are given by

$$\chi_s(0)=\frac{1}{N}\sum_{\mathbf{k}\sigma}\ \phi_s(\mathbf{k})\left(-\frac{1}{\pi}\right)\mathrm{Im}G_\sigma(+i0,\mathbf{k}) \tag{2.35}$$

and

$$\gamma=\frac{1}{3}\pi^2k_B^2\frac{1}{N}\sum_{\mathbf{k}\sigma}\ \phi_m(\mathbf{k})\left(-\frac{1}{\pi}\right)\mathrm{Im}G_\sigma(+i0,\mathbf{k})$$

$$=\frac{2}{3}\pi^2k_B^2\rho^*(0) \tag{2.36}$$

per unit cell, where

$$\rho^*(\varepsilon)=\frac{1}{N}\sum_{\mathbf{k}}\ \delta(\varepsilon-\xi(\mathbf{k})) \tag{2.37}$$

is the density of states of the quasiparticles. Equation (2.36) is divided into two parts:

$$\gamma=\tilde{\gamma}+\Delta\gamma \tag{2.38}$$

with $\tilde{\gamma}$ given by Eq. (2.34) and $\Delta\gamma$ given by

$$\Delta\gamma=\frac{1}{3}\pi^2k_B^2\frac{1}{N}\sum_{\mathbf{k}\sigma}\ \Delta\phi_m(\mathbf{k})\left(-\frac{1}{\pi}\right)\mathrm{Im}G_\sigma(+i0,\mathbf{k}). \tag{2.39}$$

Physically, $\tilde{\gamma}$ is due to the local spin fluctuations, and $\Delta\gamma$ is due to the intersite spin fluctuations.

An energy scale k_BT_Q for the quasiparticles is defined by

$$\rho^*(0)=1/(4k_BT_Q), \tag{2.40}$$

and the density of states according to Eq. (2.13) is then given by

$$\rho(0)=\frac{1+s_c}{2\tilde{\varphi}_sk_BT_K}=\frac{1}{4\phi_mk_BT_Q}. \tag{2.41}$$

Here the $\mathbf{k}$ dependence of $\phi_m(\mathbf{k})$ is ignored. The Wilson ratio is defined by

$$W_s\equiv\frac{1}{3}\pi^2k_B^2\frac{\chi_s(0)}{\gamma}=\frac{2T_Q}{T_K}\,\frac{1}{1-\alpha(0)}. \tag{2.42}$$

According to the Ward-Takahashi relation,[50,51] the expansion coefficients for the self-energies are related to the corresponding vertex functions:

$$\tilde{\varphi}_s=\frac{\tilde{\lambda}_s(0,0)}{1-U\tilde{\pi}_s(0)}=\tilde{\lambda}_s(0,0)[1+\tfrac{1}{2}U\tilde{\chi}_s(0)] \tag{2.43}$$

and

$$\phi_s(\mathbf{k})=\frac{\lambda_s(0,0;\mathbf{k},\mathbf{k})}{1-U\pi_s(0,0)}$$

$$=\lambda_s(0,0;\mathbf{k},\mathbf{k})[1+\tfrac{1}{2}U\chi_s(0,0)], \tag{2.44}$$

where Eqs. (2.14) and (2.15) have been used. We obtain

$$U\tilde{\lambda}_s(0,0)=2\tilde{\varphi}_s/\tilde{\chi}_s(0)=(1+s_c)/\rho(0) \tag{2.45}$$

and

$$U\lambda_s(0,0;\mathbf{k},\mathbf{k})=2\phi_s(\mathbf{k})/\chi_s(0,0)=1/\rho(0) \tag{2.46}$$

to leading order in k_BT_K/U. When Anderson's compensation theorem[49] is satisfied, $\tilde{\lambda}_s(0,0)=\lambda_s(0,0;\mathbf{k},\mathbf{k})$ and $\Delta\lambda_s(0,0;\mathbf{k},\mathbf{k})=0$; it is assumed in this paper that the multisite vertex function $\Delta\lambda_s(i\varepsilon_n,i\varepsilon_n+i\omega_\ell;\mathbf{k},\mathbf{k}+\mathbf{q})$ can be ignored.

Because the spin space is isotropic, the susceptibility, the polarization, and the vertex functions for the transversal spin channels are the same as those for the longitudinal spin channel.

III. INTERSITE PAIRING INTERACTION

In our starting model, Eq. (2.1), the intrasite repulsion is present only between antiparallel spins: $U_{\sigma\sigma'}=\frac{1}{2}U(1-\sigma\sigma')$, up and down spins denoted as $\sigma=\pm 1$, respectively. First, we consider an interaction with no vertex corrections as shown in Fig. 3. It is calculated in such a way that

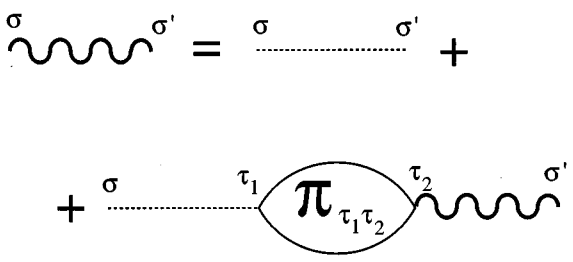

FIG. 3. Enhanced exchange interaction. While the charge channel is screened the spin channel is enhanced. A bold wavy line stands for the screened or enhanced exchange interaction, and a bubble for the irreducible polarization function.

$$V_{\sigma\sigma'}(i\omega_\ell,\mathbf{q})=U_{\sigma\sigma'}-\sum_{\tau_1\tau_2}U_{\sigma\tau_1}\pi_{\tau_1\tau_2}(i\omega_\ell,\mathbf{q})V_{\tau_2\sigma'}(i\omega_\ell,\mathbf{q})$$
$$=\tfrac{1}{2}[V_c(i\omega_\ell,\mathbf{q})-\sigma\sigma' V_s(i\omega_\ell,\mathbf{q})], \tag{3.1}$$

with $V_c(i\omega_\ell,\mathbf{q})=U/[1+U\pi_c(i\omega_\ell,\mathbf{q})]$ and

$$V_s(i\omega_\ell,\mathbf{q})=\frac{U}{1-U\pi_s(i\omega_\ell,\mathbf{q})} \tag{3.2}$$

being the interactions for the charge and the longitudinal spin channels, respectively. Next, we include the vertex corrections to obtain an interaction as shown in Fig. 4. Because only the single-site vertex functions are considered to leading order in k_BT_K/U and s_c, the intersite pairing interaction for the spin channels is given by

$$\Gamma_{\alpha\beta;\gamma\delta}(i\omega_\ell,\mathbf{q})=-\tfrac{1}{2}\tilde{\lambda}_s^2(0,0)\Big[V_s(i\omega_\ell,\mathbf{q})$$
$$-\frac{1}{N}\sum_{\mathbf{q}'}V_s(i\omega_\ell,\mathbf{q}')\Big]\sum_\eta\sigma_\eta^{\alpha\beta}\sigma_\eta^{\gamma\delta}. \tag{3.3}$$

Here $\sigma_\eta^{\alpha\beta}$ is the $(\alpha\beta)$th component of one of the three Pauli spin matrices, σ_η with $\eta=x$, y, or z. In Eq. (3.3), α and γ stand for the spins of outgoing electrons, while β and δ stand for the spins of incoming electrons. Both of the longitudinal and the transversal spin channels are included because of the isotropic property of the spin space. A total intrasite part is not studied in this paper; although it is definitely strongly repulsive because of the original strong U, it has no effects

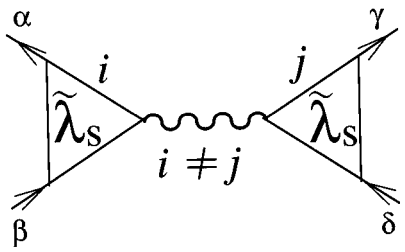

FIG. 4. Pairing interaction from the longitudinal spin channel ($\alpha=\beta$ and $\gamma=\delta$). Only the intersite part ($i\neq j$) is included. A bold wavy line stands for the intersite part of the enhanced exchange interaction.

on the T_c of the $d\gamma$-wave pairing.[9] Any intersite interaction in the charge channel is ignored because it is screened substantially.

Equation (3.2) gives

$$V_s(i\omega_\ell,\mathbf{q})=U+\tfrac{1}{2}U^2\tilde{\chi}_s(i\omega_\ell)$$
$$+\frac{1}{2}U^2\tilde{\chi}_s^2\ (i\omega_\ell)\frac{\frac{1}{4}I_s(i\omega_\ell,\mathbf{q})}{1-\frac{1}{4}I_s(i\omega_\ell,\mathbf{q})\tilde{\chi}_s(i\omega_\ell)} \tag{3.4}$$

to leading order in k_BT_K/U. Note that the first and the second terms on the right side are the single-site terms. By using Eqs. (2.45) and (3.4), Eq. (3.3) is described as

$$\Gamma_{\alpha\beta;\gamma\delta}(i\omega_\ell,\mathbf{q})=-\tilde{\varphi}_s^2\ \frac{\frac{1}{4}I_s(i\omega_\ell,\mathbf{q})}{1-\frac{1}{4}I_s(i\omega_\ell,\mathbf{q})\tilde{\chi}_s(i\omega_\ell)}\sum_\eta\ \sigma_\eta^{\alpha\beta}\sigma_\eta^{\gamma\delta} \tag{3.5}$$

to leading order in k_BT_K/U; it can also be described as

$$\Gamma_{\alpha\beta;\gamma\delta}(i\omega_\ell,\mathbf{q})=-\tilde{\varphi}_s^2\ \{\tfrac{1}{4}I_s(i\omega_\ell,\mathbf{q})$$
$$+[\tfrac{1}{4}I_s(i\omega_\ell,\mathbf{q})]^2\chi_s(i\omega_\ell,\mathbf{q})\}\sum_\eta\ \sigma_\eta^{\alpha\beta}\sigma_\eta^{\gamma\delta}. \tag{3.6}$$

The subtraction of intrasite parts is assumed in Eqs. (3.5) and (3.6). Equation (3.6) implies that when the intersite spin fluctuations are developed the intersite exchange interaction is enhanced.

Equation (2.43) shows that $\tilde{\varphi}_s$ is nothing but the reducible single-site vertex function. Equation (3.5) or (3.6) now proves that $\tilde{\varphi}_s$ is to be used as the vertex function for the spin channel argued in the Introduction: $\varphi_s=\tilde{\varphi}_s$.

Equation (3.5) or (3.6) is nothing but an intersite pairing interaction between electrons. An intersite pairing interaction between the quasiparticles is derived by including the mass renormalization, by dividing Eq. (3.5) or (3.6) by the square of the mass-renormalization factor, ϕ_m^2. Note that $(\tilde{\varphi}_s/\phi_m)^2$ plays a crucial role in the pairing interaction. We obtain

$$\tilde{\varphi}_s/\phi_m=2(1+s_c)T_Q/T_K$$
$$=(1+s_c)W_s[1-\alpha(0)] \tag{3.7}$$

from Eqs. (2.41) and (2.42); this is likely to be smaller than 2. Whether it is larger or smaller than unity depends on the interplay between the two different kinds of spin fluctuations. When the local spin fluctuations are dominant, then $T_Q\simeq T_K$; $\tilde{\varphi}_s/\phi_m\simeq 2$. When the intersite spin fluctuations are dominant, then $T_Q\ll T_K$; $\tilde{\varphi}_s/\phi_m\ll 1$.

We study now $I_s(i\omega_\ell,\mathbf{q})$ as defined by Eq. (2.21). Only the two-line diagram shown in Fig. 5 is to be considered to leading order in $1/d$; the main contribution is divided into two terms:

$$I_s(i\omega_\ell,\mathbf{q})\simeq J_s(\mathbf{q})+\Delta I_s(i\omega_\ell,\mathbf{q}). \tag{3.8}$$

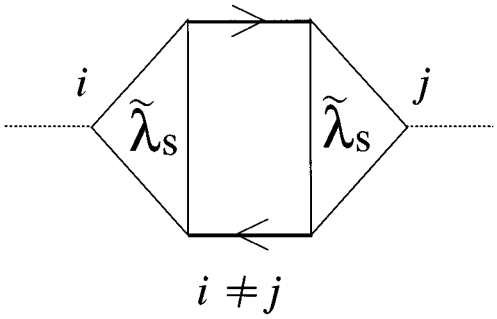

FIG. 5. There are only two intersite single-particle Green functions in the two-line multisite diagram.

The first term is the superexchange interaction due to the virtual exchange of high-energy spin excitations between the lower and upper Hubbard bands:[34]

$$J_s(\mathbf{q}) = -2J_1 \sum_{\nu=1}^{d} \cos(q_\nu a), \tag{3.9}$$

with

$$J_1 = 8t^2/(dU). \tag{3.10}$$

The second term is an exchange interaction due to that of low-energy spin excitations within the quasiparticle band; it is calculated by using Eq. (2.30) in such a way that

$$\frac{1}{4}\Delta I_s(i\omega_\ell,\mathbf{q}) = -\frac{1}{2}U^2 k_B T \frac{1}{N}\sum_{n\mathbf{k}} \left[\frac{\tilde{\lambda}_s(0,0)}{\phi_m(\mathbf{k})}\right]^2 \times \frac{1}{i\varepsilon_n - \xi(\mathbf{k})} \frac{1}{i\varepsilon_n + i\omega_\ell - \xi(\mathbf{k}-\mathbf{q})} - (\text{s.s.}) = 4c_P(k_B T_Q)^2 [P(i\omega_\ell,\mathbf{q}) - P_0(i\omega_\ell)] \tag{3.11}$$

to leading order in both $1/d$ and $k_B T_K/U$ with

$$P(i\omega_\ell,\mathbf{q}) = \frac{1}{N}\sum_{\mathbf{k}\sigma} \frac{f(\xi(\mathbf{k}+\mathbf{q})) - f(\xi(\mathbf{k}))}{\xi(\mathbf{k}) - \xi(\mathbf{k}+\mathbf{q}) - i\omega_\ell} \tag{3.12}$$

and $P_0(i\omega_\ell) = -(1/N)\Sigma_{\mathbf{q}} P(i\omega_\ell,\mathbf{q})$. Here, $-(\text{s.s.})$ means that the single-site part has to be subtracted, c_P is defined by Eq. (2.33), and $f(\varepsilon) = 1/[e^{\varepsilon/k_B T}+1]$.

Under the assumption that $I_s(+i0,\mathbf{q})$ has maxima at

$$\mathbf{Q} \equiv (\pm\pi/a, \pm\pi/a, \ldots, \pm\pi/a) \tag{3.13}$$

as $J_s(\mathbf{q})$ does and by using

$$\mathrm{Im}[4(k_B T_Q)^2 P_0(\omega+i0)] = -\frac{\pi}{2}\omega + O(\omega^3), \tag{3.14}$$

which can be derived by using Eqs. (2.37) and (2.40), $I_s(\omega+i0,\mathbf{Q}-\mathbf{q})$ is expanded in such a way that

$$\tfrac{1}{4} I_s(\omega+i0,\mathbf{Q}-\mathbf{q}) = k_B T_K \Big[\alpha(\mathbf{Q}) - \tfrac{1}{4} p_1 q^2 a^2 + i(p_2 - c_P)\frac{\pi\omega}{2k_B T_K} + \cdots \Big] \tag{3.15}$$

for small $|\omega|$ and $|\mathbf{q}|$. The imaginary term linear in ω and p_2 comes from $4c_P(k_B T_Q)^2 P(\omega,\mathbf{q})$; it is likely that $0 < p_2 \lesssim 1$. If only $J_s(\mathbf{q})$ is included, then $\alpha(\mathbf{Q}) = J_s(\mathbf{Q})/(4k_B T_K)$ and $p_1 = J_s(\mathbf{Q})/(2dk_B T_K)$. If also $\Delta I_s(i\omega_\ell,\mathbf{q})$ is included, particularly if the nesting of the Fermi surface is substantial, $\alpha(\mathbf{Q})$ and p_1 are larger than these values. In using Eqs. (2.32) and (3.15) we find that Eq. (2.20) gives

$$\chi_s(\omega+i0,\mathbf{Q}-\mathbf{q}) = \frac{\chi_s(\mathbf{Q})\kappa^2}{q^2+\kappa^2 - i\omega/\Gamma} \tag{3.16}$$

for small $|\omega|$ and $|\mathbf{q}|$ with $\chi_s(\mathbf{Q})$ defined by Eq. (2.22),

$$\kappa^2 = \frac{4[1-\alpha(\mathbf{Q})]}{p_1 a^2} \tag{3.17}$$

and

$$\Gamma = \frac{p_1}{2\pi p_2} k_B T_K a^2. \tag{3.18}$$

Thus the intersite spin fluctuations are antiferromagnetic in our model.

When $J_s(\mathbf{q})$ dominates $\Delta I_s(0,\mathbf{q})$, $I_s(0,\mathbf{q})$ can approximately be written as

$$I_s(0,\mathbf{q}) = -2I_1 \sum_{\nu=1}^{d} \cos(q_\nu a), \tag{3.19}$$

with I_1 being the nearest-neighbor component of the exchange interaction. Note that $I_1 = O(1/d)$. When the system is in the vicinity of an antiferromagnetic instability as cuprate oxides are, then $\alpha(\mathbf{Q}) \simeq 1$. It leads to $\alpha(0) \simeq -1$; the Wilson ratio, Eq. (2.42), has to be about unity or smaller.

IV. SPECIFIC HEAT DUE TO ANTIFERROMAGNETIC SPIN FLUCTUATIONS

In this section the T^2 correction to the thermodynamic potential from the intersite or antiferromagnetic spin fluctuations is studied by starting from the RSSA.

We consider a necklace diagram with $h \geq 2$ beads for the thermodynamic potential as shown in Fig. 6. It has h sections for the intersite exchange interactions and the irreducible and reducible single-site polarization functions. When the jth sections are denoted by $I_s^{[h;j]}(i\omega_\ell,\mathbf{q})$ and $\tilde{\chi}_s^{[h;j]}(i\omega_\ell)$, the contribution is described as

$$-\frac{1}{2L!} k_B T \frac{1}{N}\sum_{\ell,\mathbf{q}} \prod_{j=1}^{h} [\tfrac{1}{4} I_s^{[h;j]}(i\omega_\ell,\mathbf{q})\tilde{\chi}_s^{[h;j]}(i\omega_\ell)], \tag{4.1}$$

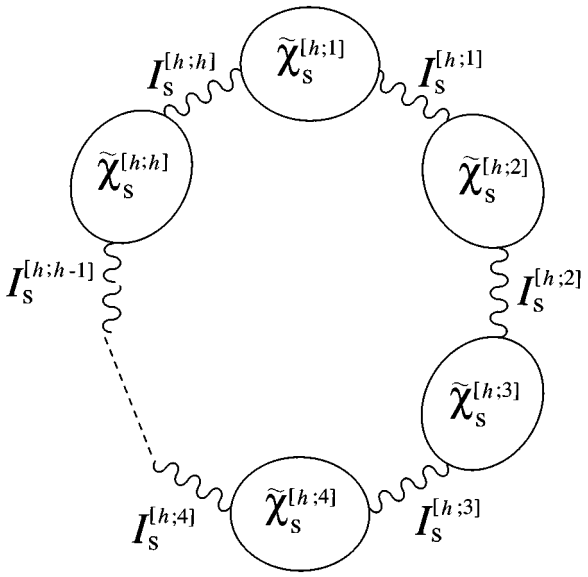

FIG. 6. Necklace diagram with $h \geq 2$ beads for the intersite thermodynamic potential. A wavy line stands for the intersite exchange interaction, and an elliptic bubble for the irreducible or reducible single-site polarization function.

with L being the order of the necklace diagram in U. The $1/L!$ appears in Eq. (4.1); the summation over the topologically same diagrams is not carried out.[52] Some sections may be the same as each other; assume, for instance, that there are r_j sections of $I_s^{(u_j)}(i\omega_\nu,\mathbf{q})$'s and s_j sections of $\tilde{\chi}_s^{(v_j)}(i\omega_\nu)$'s with u_j and v_j standing for types of sections. Then Eq. (4.1) gives

$$-\frac{1}{2L!}k_BT\frac{1}{N}\sum_{\nu,\mathbf{q}}[\tfrac{1}{4}I_s^{(u_1)}(i\omega_\nu,\mathbf{q})]^{r_1}\times[\tfrac{1}{4}I_s^{(u_2)}(i\omega_\nu,\mathbf{q})]^{r_2}\cdots[\tfrac{1}{4}I_s^{(u_j)}(i\omega_\nu,\mathbf{q})]^{r_j}\cdots\times[\tilde{\chi}_s^{(v_1)}(i\omega_\nu)]^{s_1}[\tilde{\chi}_s^{(v_2)}(i\omega_\nu)]^{s_2}\cdots[\tilde{\chi}_s^{(v_j)}(i\omega_\nu)]^{s_j}\cdots, \tag{4.2}$$

with $\Sigma_j r_j=\Sigma_j s_j=h$.

There may be more than one necklace loop in the diagram. As far as we are concerned with the T^2 correction, we have to consider *independently* the summation over ω_ν appearing along each necklace loop by replacing the other summations by the corresponding integrations at $T=0$ K; the T^2 correction comes only from the summation over imaginary energies, for example, the summation over ω_ν, and the explicit temperature dependence of $I_s^{(u_i)}(i\omega_\nu,\mathbf{q})$'s and $\tilde{\chi}_s^{(v_i)}(i\omega_\nu)$'s can be ignored in Eq. (4.2).

We then count the number of diagrams having the same T^2 correction as Eq. (4.2). In the imaginary-time representation, L imaginary times, τ_1, τ_2, . . . , τ_L, appear in the diagram; the permutation among the L τ's results in a factor $L!$. This is obviously overcounting, however; we are concerned with the circular permutation. One of the sections has to be fixed; this gives rise to a factor $1/h$. The permutation over the h polarization functions and the h intersite exchange interactions give factors $h!/(r_1!r_2!\cdots r_j!\cdots)$ and $h!/(s_1!s_2!\cdots s_j!\cdots)$, respectively. Thus we obtain

$$L!\frac{1}{h}\frac{h!}{r_1!r_2!\cdots r_j!\cdots}\frac{h!}{s_1!s_2!\cdots s_j!\cdots} \tag{4.3}$$

as the total number of diagrams.

The T^2 correction is given by

$$\begin{aligned}\Delta\Omega' &= -\frac{3}{2}k_BT\frac{1}{N}\sum_{\nu,\mathbf{q}}\sum_{h=2}^{+\infty}\frac{1}{h}\sum_{\{r\}}\frac{h!}{r_1!r_2!\cdots r_j!\cdots}[\tfrac{1}{4}I_s^{(u_1)}(i\omega_\nu,\mathbf{q})]^{r_1}[\tfrac{1}{4}I_s^{(u_2)}(i\omega_\nu,\mathbf{q})]^{r_2}\cdots\\ &\quad\times\left[\frac{1}{4}I_s^{(u_j)}(i\omega_\nu,\mathbf{q})\right]^{r_j}\cdots\sum_{\{s\}}\frac{h!}{s_1!s_2!\cdots s_j!\cdots}[\tilde{\chi}_s^{(v_1)}(i\omega_\nu)]^{s_1}[\tilde{\chi}_s^{(v_2)}(i\omega_\nu)]^{s_2}\cdots[\tilde{\chi}_s^{(v_j)}(i\omega_\nu)]^{s_j}\cdots\\ &= -\frac{3}{2}k_BT\frac{1}{N}\sum_{\nu,\mathbf{q}}\sum_{h=2}^{+\infty}\frac{1}{h}[\tfrac{1}{4}I_s(i\omega_\nu,\mathbf{q})\tilde{\chi}_s(i\omega_\nu)]^h.\end{aligned} \tag{4.4}$$

Here the sums over $\{r\}$ and $\{s\}$ are over all the possible combinations of r_j's and s_j's, respectively, and the two relations

$$I_s^h(i\omega_\nu,\mathbf{q})=\sum_{r_1+r_2+\cdots+r_j+\cdots=h}\frac{h!}{r_1!r_2!\cdots r_j!\cdots}[I_s^{(u_1)}(i\omega_\nu,\mathbf{q})]^{r_1}[I_s^{(u_2)}(i\omega_\nu,\mathbf{q})]^{r_2}\cdots[I_s^{(u_j)}(i\omega_\nu,\mathbf{q})]^{r_j}\cdots \tag{4.5}$$

and

$$\tilde{\chi}_s^h(i\omega_\nu)=\sum_{s_1+s_2+\cdots+s_j+\cdots=h}\frac{h!}{s_1!s_2!\cdots s_j!\cdots}[\tilde{\chi}_s^{(v_1)}(i\omega_\nu)]^{s_1}[\tilde{\chi}_s^{(v_2)}(i\omega_\nu)]^{s_2}\cdots[\tilde{\chi}_s^{(v_j)}(i\omega_\nu)]^{s_j}\cdots \tag{4.6}$$

are used. In Eq. (4.4) the factor of 3 is included because of the transversal and the longitudinal spin channels. Because of $(1/N)\Sigma_{\mathbf{q}} I_s(i\omega_{\not\prime},\mathbf{q})=0$, the summation over h in Eq. (4.4) can be made for $h=1$:

$$\Delta\Omega'(T)=\frac{3}{2}\int_{-\infty}^{+\infty} d\omega[2n(\omega)+1] \times\frac{1}{2\pi N}\sum_{\mathbf{q}} \mathrm{Im}\{\ln[1-\tfrac{1}{4}I_s(\omega+i0,\mathbf{q})\widetilde{\chi}_s(\omega+i0)]\}, \tag{4.7}$$

with $n(\omega)=1/[e^{\omega/k_BT}-1]$. Note that $\Delta\Omega'(T)$ is of higher order in $1/d$.

Using Eq. (2.20) we obtain

$$1-\tfrac{1}{4}I_s(\omega+i0,\mathbf{q})\widetilde{\chi}_s(\omega+i0)\simeq\frac{4}{I_s(+i0,\mathbf{Q})\chi_s(\omega+i0,\mathbf{q})} \tag{4.8}$$

for small $|\omega|$ and $|\mathbf{q}-\mathbf{Q}|$. Using Eq. (3.16) we find that the T^2 correction in two dimensions $(d=2)$ is given by

$$\begin{aligned}\Delta\Omega(T)&\equiv\Delta\Omega'(T)-\Delta\Omega'(0)\\ &=-\frac{3a^2}{4\pi^2}\int_0^{+\infty} d\omega n(\omega)\int_0^{q_c^2} dq^2\tan^{-1}\left(\frac{\omega/\Gamma}{q^2+\kappa^2}\right)\\ &=-\frac{k_B}{2T_0}T^2\ln\sqrt{(q_c/\kappa)^2+1}+O(T^4),\end{aligned} \tag{4.9}$$

with q_c being a cutoff wave number and

$$k_BT_0\equiv\frac{2\Gamma}{a^2}=\frac{p_1}{\pi p_2}k_BT_K \tag{4.10}$$

an energy scale for the antiferromagnetic spin fluctuations. The intersite specific-heat coefficient is given by

$$\Delta\gamma=-\frac{\partial^2\Delta\Omega(T)}{\partial T^2}=\frac{k_B}{T_0}\ln\sqrt{(q_c/\kappa)^2+1}. \tag{4.11}$$

It is nothing but $\Delta\gamma$ as given by Eq. (2.39).

V. APPLICATION TO CUPRATE OXIDES

A. Heavy quasiparticles

The theoretical framework of this paper includes a long self-consistency procedure as is discussed in Appendix A; we do not try to complete it. It is shown in this section that experimental data for the normal state of cuprate oxides are consistent with the Fermi-liquid relations studied in the previous sections. It is then argued that a pairing interaction deduced from the experimental data is strong enough to reproduce the observed critical temperatures of $T_c\simeq 100$ K.

The essential physics are presumably almost the same for the different cuprate oxides except for electron doped cuprate oxides like $Nd_{2-x}Ce_xCuO_{4-\delta}$; we consider $YBa_2Cu_3O_{7-\delta}$ with $T_c\simeq 90$ K as an example. The cuprate oxides are in the vicinity of an antiferromagnetic instability. Considering that the intersite exchange interaction has small distant-neighbor components as well as a large nearest-neighbor component we assume that $\alpha(\mathbf{Q})\simeq 0.9$ and $1-\alpha(0)\simeq 1.8$ as is implied by the last argument in Sec. III.

Using an experimental specific-heat coefficient[4] of $\gamma\simeq 14$ mJ/K^2 CuO_2 mol together with Eqs. (2.36) and (2.40) we find

$$k_BT_Q\simeq 8.4\times10^{-2}\ \text{eV} \tag{5.1}$$

as the energy scale for the quasiparticles. Because the spin-orbit interaction is weak on Cu ions, the effective g factor is nearly equal to 2; we use $g=3\sqrt{g_{ab}^2 g_c}\simeq 2.17$ with $g_{ab}=2.07$ and $g_c=2.37$ being the effective g factors along and perpendicular to the CuO_2 planes, respectively.[53] Using an experimental susceptibility[53] of $\frac{1}{4}g^2\mu_B^2\chi_s(0)\simeq 9.0\times10^{-5}$emu/$CuO_2$ mol we find

$$W_s\simeq 0.40 \tag{5.2}$$

as the Wilson ratio. Using Eq. (3.7) together with $1-\alpha(0)\simeq 1.8$ we obtain $k_BT_K\simeq 0.23$ eV and

$$\widetilde{\varphi}_s/\phi_m=2T_Q/T_K\simeq 0.72. \tag{5.3}$$

This tells that both the local and the antiferromagnetic spin fluctuations are responsible for the formation of the heavy quasiparticles.

Using Eqs. (2.34), (2.38), and (4.11) together with $\widetilde{\varphi}_s/\widetilde{\phi}_m=2$ we obtain

$$k_BT_0\frac{\pi^2}{6\ln\sqrt{(\kappa_c/\kappa)^2+1}}=\frac{k_BT_KT_Q}{T_K-T_Q}\simeq 0.13\ \text{eV}. \tag{5.4}$$

We define another energy scale of the antiferromagnetic spin fluctuations by

$$k_BT_A\equiv\frac{2\pi}{\chi_s(\mathbf{Q})\kappa^2a^2}=\frac{\pi}{2}p_1k_BT_K \tag{5.5}$$

in addition to k_BT_0. An analysis of normal-state properties[65,66] gives $k_BT_0=0.1$–0.2 eV and $k_BT_A=0.5$–0.7 eV; their ratio is $T_0/T_A=0.2$–0.4, while $T_0/T_A=2/(\pi^2p_2)$ according to Eqs. (4.10) and (5.5). We obtain $0.5\lesssim p_2\lesssim 1$; this p_2 is reasonable as is discussed in Sec. III. Using Eq. (5.5) we obtain $1.5\lesssim p_1\lesssim 2$; p_1 larger than unity implies that the nesting of the Fermi surface is substantial. Using Eq. (3.17) together with $\alpha(\mathbf{Q})\simeq 0.9$ and $1.5\lesssim p_1\lesssim 2$ we obtain $1/\kappa\simeq 2a\simeq 8$ Å; this $1/\kappa$ is consistent with an observed magnetic correlation length of about 10 Å.[20] Also $k_BT_0=0.1$–

0.2 eV is consistent with Eq. (5.4), and it is also consistent with Eq. (4.10), if $1.5 \lesssim p_1 \lesssim 2$, $0.5 \lesssim p_2 \lesssim 1$, and $k_B T_K \simeq 0.23$ eV are used.

B. Pairing interaction

Using Eq. (3.10) we obtain $J_1 = 4t^2/(dU) \simeq 0.13$ eV for $d=2$, $|t| \simeq 0.5$ eV, and $U \simeq 8$ eV. This is consistent with the experimental $J_1 = 0.1$–0.15 eV.[19,20] Equation (3.12) is expanded into a Fourier series:

$$[P(\omega + i0, \mathbf{q})]_{\omega=0} = \frac{1}{8 k_B T_Q} \{ b_0 - b_1 \times [\cos(q_x a) + \cos(q_y a)] + \cdots \}, \quad (5.6)$$

where the first term proportional to b_0 is the intrasite part, the second term proportional to b_1 is the nearest-neighbor part, and so on. By assuming that

$$\xi(\mathbf{k}) \simeq -k_B T_Q [\cos(k_x a) + \cos(k_y a)] + \text{const}, \quad (5.7)$$

the constant b_1 is estimated to be $b_1 \simeq 0.5$ very close to half filling, for instance, from Fig. 10(a) of Ref. 54. What mainly determines b_1 is the whole band structure of the quasiparticles: The nesting of the Fermi surface plays a minor role. We then obtain

$$I_1 \simeq J_1 + b_1 k_B T_Q \simeq 0.18 \text{ eV} \quad (5.8)$$

for the static and nearest-neighbor component of the exchange interaction.

Equation (5.8) leads to $I_1 / k_B T_K \simeq 0.8$; this is consistent with the assumption of $\alpha(\mathbf{Q}) \simeq 0.9$ and $1 - \alpha(0) \simeq 1.8$ made in Sec. V. A. The exchange interaction between distant sites has to be included in order to obtain an accurate numerical value for $\alpha(\mathbf{Q})$.

The static part of the exchange interaction is approximately given by Eq. (3.19) together with Eq. (5.8). The enhanced exchange interaction in Eq. (3.5) is expanded into a Fourier series:

$$\left[\frac{\frac{1}{4} I_s(\omega + i0, \mathbf{q})}{1 - \frac{1}{4} I_s(\omega + i0, \mathbf{q}) \tilde{\chi}_s(\omega + i0)} \right]_{\omega=0} = \frac{1}{4} I_1 \{ c_0(\zeta) - 2 c_1(\zeta) [\cos(q_x a) + \cos(q_y a)] + \cdots \}, \quad (5.9)$$

with $\zeta \equiv I_1 / k_B T_K$. The first term proportional to $c_0(\zeta)$ is the intrasite part; it plays no role for the $d\gamma$-wave Cooper pairing. The second term proportional to

$$c_1(\zeta) = \frac{1}{\pi^2} \int_0^\pi dx \int_0^\pi dy \frac{(\cos x + \cos y)^2}{1 + (\zeta/2)(\cos x + \cos y)} = \sum_{n=0}^{\infty} \frac{2(2n+1)!!}{(2n+2)!!} \zeta^{2n} \quad (5.10)$$

is the enhanced interaction between the nearest neighbors. It is trivial that $c_1(0) = 1$. Note that it can be as large as two; for example, $c_1(0.9) = 2.2313 \ldots$.

The static part of the pairing interaction between the nearest neighbors is estimated to be as large as

$$I_1 c_1(0.8) (\tilde{\varphi}_s / \phi_m)^2 \simeq 0.15 \text{ eV} \quad (5.11)$$

by including $(\tilde{\varphi}_s / \phi_m)^2 \simeq 0.52$, which comes from the vertex renormalization and the mass renormalization. Here $c_1(0.8) = 1.689 \ldots$ is used; $I_1 / k_B T_K \simeq 0.8$.

The energy scale of the superexchange interaction is the energy difference between the lower and upper Hubbard bands; it is much larger than the quasiparticle bandwidth. The superexchange interaction is almost instantaneous for the quasiparticles. The energy scale of the exchange interaction and the energy scale of the enhanced part of the pairing interaction are certainly small for particular $\mathbf{q}$ components; for example, the energy scale of the enhanced part is $\Gamma \kappa^2 = \frac{1}{2} k_B T_0 (\kappa a)^2 = 1 \times 10^{-2}$–$2 \times 10^{-2}$ eV for $\mathbf{q} \simeq Q$. However, the energy scale of the nearest-neighbor components is not $\Gamma \kappa^2$ but $k_B T_Q$; almost all the $\mathbf{q}$ components play a role. Therefore, the above argument from Eqs. (5.6)–(5.11) is valid not only for $\omega = 0$ but also for $|\omega| \ll k_B T_Q$.

When the bandwidth of the quasiparticles and the pairing interaction between the quasiparticles are given, it is straightforward to solve the gap equation. Actually the gap equation has already been solved in Ref. 8, where a cutoff energy θ, corresponding to the Debye cutoff energy in the Bardeen-Cooper-Schrieffer (BCS) theory,[55] was treated as a parameter. Figure 2 of Ref. 8 proves that as long as θ is larger than ~ 0.05 eV which is smaller than $k_B T_Q$ the θ dependence of critical temperatures is small;[56] the energy dependence of the pairing interaction cannot play any essential role in the cuprate oxides.

Figure 2 of Ref. 8 also shows that for a pairing interaction as large as 0.15 eV, as is given by Eq. (5.11), the critical temperatures are $T_{c0} \simeq 200$ K for the $d\gamma$-wave pairing in the absence of any pair breaking. They are about twice as high as is observed for $YBa_2Cu_3O_{7-\delta}$. The discrepancy between theory and experiment may be resolved, when the pair-breaking effect of the antiferromagnetic spin fluctuations is considered.

The phase relaxation time $\tau(T)$ of the quasiparticles is estimated to be as large as $\hbar / \tau(T) \simeq 1.3 k_B T$ above $T_c \simeq 90$ K.[57] A simple application of Abrikosov and Gorkov's theory[58] tells that $T_{c0} \simeq 200$ K's are reduced to $T_c \simeq 90$ K's because $\hbar / [2\pi \tau(T) k_B T_{c0}] \simeq 0.21$ for $T \simeq T_c$ and $T_{c0} \simeq 2 T_c$. It is interesting to confirm that such a temperature dependence of $\tau(T)$ is actually reproduced by considering scattering by the antiferromagnetic spin fluctuations.

Because the pair-breaking effect is weak at $T = 0$ K, the gaps at $T = 0$ K, $\varepsilon_G(0)$, have to be as large as those in the absence of any pair breaking. According to the BCS theory[55] $\varepsilon_G(0) / k_B T_c = 3.53$ for the isotropic s-wave pairing. Two numbers have been calculated for the $d\gamma$-wave pairing: $\varepsilon_G(0) / k_B T_c = 4.35$ in Ref. 8 and $\varepsilon_G(0) / k_B T_c = 4.27$ in Ref. 59.[60] Then our prediction is $\varepsilon_G(0) / k_B T_c \simeq 4 T_{c0} / T_c \simeq 8$. Actually many experiments imply that $\varepsilon_G(0) / k_B T_c \simeq 8$: the tunneling experiment,[61] the Raman-scattering experiment,[62] the photoemission experiment,[63] and the infrared absorption experiment.[64]

VI. DISCUSSION

We have confined ourselves to studying the Hubbard model. It is straightforward to extend the study of this paper to the periodic Anderson Hamiltonian (PAM), which is an effective Hamiltonian for Kondo lattices or the so-called heavy-electron liquids. It is trivial that almost the same results are obtained for the PAM as those in this paper; Eq. (2.20) together with Eq. (2.21) confirms a naive physical picture for Kondo lattices: Spin fluctuations localized at each site interact with each other by an exchange interaction. The Hubbard model in the vicinity of the Mott transition is another effective Hamiltonian for Kondo lattices. Because of the similarity between the Hubbard model and the PAM and because of the moderately large mass-renormalization factor of cuprate oxides, it is reasonable to classify cuprate oxides into the heavy-electron liquids of moderately heavy quasiparticles.

Because the superexchange interaction cannot be appreciably different within the single-band Hubbard model, it is difficult to explain different T_c and different Néel temperatures T_N in different cuprate oxides. The virtual exchange of spin excitations between a pair of bands far from the chemical potential may also cause an exchange interaction. Its different contributions may explain different T_c and different T_N in different cuprate oxides. It is interesting to examine the correlation between experimental T_c and T_N.

The second term within the curly bracket of Eq. (3.6) is similar to the pairing interaction, $-I^2\chi_s(i\omega_\nearrow,\mathbf{q})$, of the spin-fluctuation mechanism.[66] According to Eq. (3.6) the phenomenological intrasite repulsion I is approximately given by $I\simeq(1/4)I_s(0,\mathbf{Q})$.

Moriya and Ueda[66] have argued that the observed T_c as high as 100 K are reproduced by using an experimental $\chi_s(\omega+i0,\mathbf{q})$ together with $I\simeq 0.7$ eV and $W\simeq 1$ eV with W being the quasiparticle bandwidth. Their theory is improved in the following way. First of all, the factor of 3 appears because of the transversal channels and the longitudinal channel. A factor $(\tilde{\varphi}_s/\phi_m)^2\simeq 0.52$ appears because of the vertex renormalization and the mass renormalization. The phenomenological I and the bandwidth W are replaced by $\frac{1}{4}I_s(0,\mathbf{Q})\simeq I_1\simeq 0.18$ eV and $4k_BT_Q\simeq 0.34$ eV, respectively. Then the coupling constant is reduced by

$$3(\tilde{\varphi}_s/\phi_m)^2(I_1/I)^2(W/4k_BT_Q)\simeq 0.3. \tag{6.1}$$

This result is consistent with the conclusion of this paper that about a third of the pairing interaction is due to the enhanced part.

It is necessary to improve the phenomenological theories[65,66] to explain anomalous properties of cuprate oxides more quantitatively. On the other hand, certain anomalies have already been explained essentially by the $1/d$ expansion method.[8,67–72]

Superconducting gaps for the pure $d\gamma$-wave Cooper pairs have nodal lines. However, certain experiments suggest that anisotropic gaps with no node are open at $T\ll T_c$: the almost temperature-independent penetration depth[73,74] and the tunneling spectra.[75] As is argued in the Introduction T_c cannot be as high as 100 K except for the $d\gamma$-wave pairing; even if gaps with no node actually open in some cuprate oxides, the high-T_c superconductivity is to be explained in terms of a little modified but essentially $d\gamma$-wave pairing. For example, it has been pointed out[76] that gaps with no node can open below the second superconducting critical temperature T_{c2} in distorted lattices where the admixture of an s-wave component is substantial. It has been argued[77,78] that certain modes of phonons show softening at T_{c2}. A sharp but tiny anomaly of the transversal nuclear quadrupole relaxation (NQR) rate of Cu nuclei in the CuO_2 planes is observed at about 35 K in $YBa_2Cu_3O_{7-\delta}$ with $T_c\simeq 90$ K.[79–82] The anomaly together with no anomaly of the transversal NQR of Cu nuclei in the CuO chains and no anomaly of the longitudinal NQR implies that the softening of phonons occurs in the cuprate oxides. It is interesting to examine the anomaly in detail.

VII. CONCLUSION

The Fermi-liquid theory is developed for the Hubbard model. The local and quantal spin fluctuations, which are of leading order in $1/d$ with d being the spatial dimensionality, are totally included in the renormalized single-site approximation (RSSA). Solving the Hubbard model in the RSSA is reduced to solving the Anderson model; the local Kondo temperature T_K is defined as the temperature or energy scale of the local spin fluctuations. Another small parameter is k_BT_K/U with k_B being the Boltzmann constant and U the intrasite repulsion. The intersite or antiferromagnetic spin fluctuations are considered perturbatively in terms of $1/d$ and to leading order in k_BT_K/U. The two different kinds of spin fluctuations are responsible for the formation of the quasiparticles; another energy scale T_Q is defined in such a way that the density of states of the quasiparticles is $1/(4k_BT_Q)$ at the chemical potential per spin and unit cell.

The two exchange interactions are responsible for the $d\gamma$-wave Cooper pairing as well as the development of the antiferromagnetic spin fluctuations: the superexchange interaction and the exchange interaction due to the virtual exchange of spin excitations within the quasiparticle band. The development of the antiferromagnetic spin fluctuations has both the reduction and the enhancement effects on the pairing mechanism: the reduction of the vertex function divided by the mass-renormalization factor and the enhancement of the exchange interactions. The enhanced part of the exchange interactions is similar to the pairing interaction of the phenomenological spin-fluctuation mechanism.

The Fermi-liquid theory applies to $YBa_2Cu_3O_{7-\delta}$ with $T_c\simeq 90$ K. Their quasiparticle bandwidth is $4k_BT_Q\simeq 0.34$ eV according to the specific-heat coefficient of 14 mJ/K^2 CuO_2 mol. Their Wilson ratio is estimated to be about 0.40 from the specific-heat coefficient and the susceptibility of about 9.0×10^{-5} emu/CuO_2 mol. The large specific-heat coefficient and the small Wilson ratio tell that both the local and the antiferromagnetic spin fluctuations are responsible for the formation of the heavy quasiparticles, and that the reduction effect is so substantial that $(\tilde{\varphi}_s/\phi_m)^2\simeq 0.52$ with $\tilde{\varphi}_s$ being the single-site vertex function and ϕ_m the mass-renormalization factor. The nearest-neighbor component of the exchange interactions is estimated to be about 0.18 eV; about 0.13 eV is due to the superexchange interaction, and about 0.05 eV is due to the novel exchange interaction. It is enhanced to being about 1.5 times as large as its bare exchange interaction. The eventual Cooper-pairing interaction

estimated by including both the reduction and the enhancement effects is strong enough to give critical temperatures as high as $T_{c0} \simeq 200$ K for the $d\gamma$-wave pairing in the absence of any pair breaking. There is experimental evidence that the pair-breaking effect of the antiferromagnetic spin fluctuations reduces $T_{c0} \simeq 200$ K down to $T_c \simeq 90$ K. In conclusion, the interplay between the local and the intersite spin fluctuations plays the crucial role in the mechanism of the high-temperature superconductivity of the cuprate oxides.

ACKNOWLEDGMENT

This work was partly supported by Grant-in-Aid for Scientific Research (C) No. 08640434 from the Ministry of Education, Science, Sports and Culture of Japan.

APPENDIX A: UNPERTURBED STATE OF THE 1/*d* EXPANSION METHOD

The theoretical framework of this paper includes a long self-consistency procedure. Given an input of the single-site and the multisite self-energies we compute the dispersion relation of the quasiparticles, the dynamical susceptibility, the intersite exchange interaction, and then the multisite self-energy by the 1/*d* expansion method. In the nest step the single-site self-energy is calculated in the RSSA. We thus obtain an output of the single-site and the multisite self-energies from this procedure; this output should be identical to the input.

The RSSA depends on the multisite self-energy as is discussed in Sec. II. Effects of the multisite self-energy on the RSSA can approximately be included by using a slightly different unrenormalized dispersion relation from the original one, Eq. (2.2). According to the Gutzwiller approximation,[25] which is one of the simplest SSA's, the mass-renormalization factor scarcely depends on the unrenormalized dispersion relation. It is approximately given by $\tilde{\phi}_m \simeq 1/|1-n|$, with n being the number of electrons per unit cell. In Ref. 28 another SSA also gives a similar result. The finite $\tilde{\phi}_m$ means that the local Kondo temperature is nonzero; the solution of the RSSA is of Landau's normal Fermi liquid. The unperturbed state of the 1/*d* expansion method is the Fermi liquid for non-half-filling.

The mapping condition (2.12) is equivalent to the condition that the hybridization energy $\Delta(\varepsilon)$ of the Anderson model be given by[33,41]

$$\Delta(\varepsilon) = \mathrm{Im}[1/R_{ii\sigma}(\varepsilon + i0) + \tilde{\Sigma}_\sigma(\varepsilon + i0)]. \qquad \text{(A1)}$$

It cannot be negative.[41] When $\Delta'(\varepsilon) = \Delta(\varepsilon) + \delta\Delta$, with $\delta\Delta$ being a nonzero and infinitesimally small positive energy, is used instead of $\Delta(\varepsilon)$ in solving the MAM, the solution of the RSSA is of Landau's normal Fermi liquid for any filling without fail. We had best use this Fermi liquid as the unperturbed state.

In almost all the effective Hamiltonians, however, their ground states are not Landau's Fermi liquids. This fact never means the breakdown of the 1/*d* expansion theory of this paper. It is straightforward to extend it in a way that allows us to treat the ground state with an order parameter and its excited states. *In general, Landau's normal Fermi liquid is a starting point in examining more interesting lower-temperature phases.*

APPENDIX B: ABSENCE OF THE PARAMAGNETIC MOTT TRANSITION

A sophisticated question for the single-band Hubbard model is whether or not a metal-insulator transition, a paramagnetic Mott transition, occurs at $T=0$ K within the SSA when $U/|t|$ is increased.[43–46] This question is concerned with excited states; the ground state is antiferromagnetic or superconducting, at least, in the large-U regime.[40] An answer to the question depends on the Hilbert space to which the excited states are restricted.

First of all, the paramagnetic Mott transition does not occur for non-half-filling as is discussed in Appendix A. We therefore confine ourselves to examining the just half filling.

Restrict the Hilbert space to zero-entropy states by using $\Delta'(\varepsilon) = \Delta(\varepsilon) + \delta\Delta$ as defined in Appendix A. The lowest-energy state under this restriction is the Fermi liquid; a paramagnetic Mott transition does not occur. However, as empty and doubly occupied sites are never completely excluded, the Fermi liquid is not likely to be the lowest-energy state within the SSA, at least, in the large-U limit. Then another plausible restriction is that the lowest-energy state are to be looked for simply within the SSA.

First, we consider a model whose unrenormalized electron density of states has infinitely long tails like a Gaussian or a Lorentzian. The paramagnetic Mott transition is unlikely to occur; empty and doubly occupied states are never completely excluded.[46] When the density of states is of a Lorentzian shape, in particular, $\Delta(\varepsilon)$ defined by Eq. (A1) is nonzero and independent of ε;[83] the paramagnetic Mott transition does not occur definitely. The lowest-energy state within the SSA is the normal Fermi liquid.

Second, we consider another model whose unrenormalized density of states has sharp edges like a semielliptic shape.[44] In the small-U limit the solution of the SSA is of the normal Fermi liquid. Its entropy is zero. In the large-U limit, on the other hand, the solution of the SSA is of a paramagnetic Mott insulator. Empty and doubly occupied sites are totally excluded, and its entropy is nonzero.[44] The paramagnetic Mott insulator is a high-temperature phase in a sense; homogeneity is restored by the thermal average at $T=0$ K. The transition occurs at a critical $U=U_c$. It is of the first order at $T=0$ K; it is presumably reduced to a crossover at elevated temperatures. This is nothing but the conventional physical picture of the Mott transition. Note, however, that this transition occurs only at the *just* half filling and that the paramagnetic Mott insulator is never the ground state within the single-band Hubbard model.

The strong correlations between electrons cannot explain by themselves actual metal-insulator transitions of the first order, which occur even for non-half-filling. However, it seems to be certain that the strong correlations play a crucial role. It is interesting to examine which effect also plays a crucial role among an electron-phonon interaction or a magnetostriction effect in paramagnetic phases, the existence of multiple bands, and other effects.

[1] J. G. Bednorz and K. A. Müller, Z. Phys. B **64**, 189 (1986).
[2] L. D. Landau, Sov. Phys. JETP **3**, 920 (1956).
[3] As is discussed in Appendix A this assumption is valid within the theoretical framework of the $1/d$ expansion method.
[4] See, for example, A. Junod, T. Graf, D. Saches, G. Triscone, and J. Müller, Physica B **165-166**, 1335 (1990).
[5] A. Migdal, Sov. Phys. JETP **7**, 996 (1958).
[6] J. E. Hirsch, Phys. Rev. Lett. **54**, 1317 (1985).
[7] P. W. Anderson, Science **235**, 2 (1987).
[8] F. J. Ohkawa, J. Phys. Soc. Jpn. **56**, 2267 (1987). Different notations are used in this reference. For example, $-4J_s^*=-4J\chi_s^2(\mathbf{k})/\chi_m^2(\mathbf{k})$ corresponds to $J_1(\varphi_s/\phi_m)^2$ or $I_1c_1(\zeta)(\tilde{\varphi}_s/\phi_m)^2$ of this paper.
[9] An effective intrasite repulsion is different from the original U. It corresponds to the kinetic-energy increase of electrons keeping away from each other because of the strong U; the effective intrasite repulsion between the quasiparticles is presumably of the order of the quasiparticle bandwidth. If an intrasite attraction were introduced instead of the intrasite repulsion T_c's of s-wave pairing could be high.
[10] F. J. Ohkawa, Phys. Rev. B **42**, 4163 (1990).
[11] J. T. Markert, T. W. Noh, S. E. Russek, and R. M. Cotts, Solid State Commun. **63**, 847 (1987).
[12] M. Mali, D. Brinkmann, L. Pauli, J. Roos, and H. Zimmermann, Phys. Lett. A **124**, 112 (1987).
[13] W. W. Warren, Jr., R. E. Walsted, G. F. Brennert, G. P. Espinosa, and J. P. Remeika, Phys. Rev. Lett. **59**, 1860 (1987).
[14] P. C. Hammel, M. Takigawa, R. H. Heffner, Z. Fisk, and K. C. Ott, Phys. Rev. Lett. **63**, 1992 (1989).
[15] W. N. Hardy, D. A. Bonn, D. C. Morgan, R. Liang, and K. Zhang, Phys. Rev. Lett. **70**, 3999 (1993).
[16] Z.-X Shen, D. S. Dessau, B. O. Wells, D. M. King, W. E. Spicer, A. J. Arko, D. Marshall, L. W. Lombardo, A. Kapitulink, P. Dickinson, S. Doniach, J. Dicarlo, A. G. Loeser, and C. H. Park, Phys. Rev. Lett **70**, 1553 (1993).
[17] M. Sirgrist and T. M. Rice, J. Phys. Soc. Jpn. **61**, 4283 (1992).
[18] D. A. Wollman, D. J. van Harlinger, W. C. Lee, D. M. Ginsberg, and A. J. Legget, Phys. Rev. Lett. **71**, 2134 (1993).
[19] K. B. Lyons, P. A. Fleury, L. F. Schneemeyer, and J. V. Waszczak, Phys. Rev. Lett. **60**, 732 (1988).
[20] J. Rossat-Mignod, L. P. Regnault, C. Vettier, P. Burlet, J. Y. Henry, and G. Lanpertot, Physica **169**, 58 (1991).
[21] K. G. Wilson, Rev. Mod. Phys. **47**, 773 (1995).
[22] P. Nozières, J. Low Temp. Phys. **17**, 31 (1995).
[23] K. Yamada, Prog. Theor. Phys. **53**, 970 (1975).
[24] K. Yosida and K. Yamada, Prog. Theor. Phys. **53**, 1286 (1975).
[25] M. C. Gutzwiller, Phys. Rev. Lett. **10**, 159 (1963).
[26] J. Hubbard, Proc. R. Soc. (London) A **276**, 238 (1963).
[27] It is remarkable that another distinguished theory has been proposed in 1963: J. Kanamori, Prog. Theor. Phys. **30**, 275 (1963).
[28] F. J. Ohkawa, J. Phys. Soc. Jpn. **58**, 4156 (1989).
[29] Y. Kuramoto and T. Watanabe, Physica **148B**, 80 (1987).
[30] W. Metzner and D. Vollhardt, Phys. Rev. Lett. **62**, 324 (1989).
[31] F. J. Ohkawa, Phys. Rev. B **44**, 6812 (1991).
[32] F. J. Ohkawa, J. Phys. Soc. Jpn. **60**, 3218 (1991).
[33] F. J. Ohkawa, J. Phys. Soc. Jpn. **61**, 1615 (1992).
[34] F. J. Ohkawa and N. Matsumoto, J. Phys. Soc. Jpn. **63**, 602 (1994).
[35] In general, the multisite terms include intrasite terms. Thus we use *multisite* in this paper instead of *intersite* in the previous papers Ref. 31–33.
[36] H. Shiba, Prog. Theor. Phys. **54**, 967 (1975).
[37] N. Andrei, K. Furuya, and J. H. Lowenstein, Rev. Mod. Phys. **55**, 331 (1983).
[38] A. M. Tsvelick and P. B. Wiegmann, Adv. Phys. **32**, 453 (1983).
[39] A. Okiji and N. Kawakami, *Theory of Heavy Fermions and Valence Fluctuations*, Springer Series in Solid-State Science Vol. 62 (Springer-Verlag, Berlin, 1985), p. 46.
[40] F. J. Ohkawa, J. Phys. Soc. Jpn. **61**, 4521 (1992).
[41] F. J. Ohkawa, J. Phys. Soc. Jpn. **61**, 4490 (1992).
[42] The RSSA can be extended to be able to treat the spin and site dependent self-energy. If, for instance, the spin-dependent self-energy is considered, the RSSA is rigorous for ferromagnetic phases.
[43] M. Jarrell, Phys. Rev. Lett. **69**, 168 (1992).
[44] A. Georges and W. Krauth, Phys. Rev. Lett. **69**, 1240 (1992).
[45] X. Y. Zhang, M. J. Rozenberg, and G. Kotliar, Phys. Rev. Lett. **70**, 1666 (1993).
[46] Th. Pruschke, D. L. Cox, and M. Jarrell, Phys. Rev. B **47**, 3553 (1993).
[47] J. M. Luttinger and J. C. Ward, Phys. Rev. **118**, 1417 (1960).
[48] J. M. Luttinger, Phys. Rev. **119**, 1153 (1960).
[49] P. W. Anderson, Phys. Rev. **124**, 41 (1961).
[50] J. C. Ward, Phys. Rev. **78**, 182 (1950).
[51] Y. Takahashi, Nuovo Cimento **6**, 370 (1957).
[52] Reversing the $(L-1)$ U lines is considered in Eq. (4.1); it gives a factor 2^{L-1}.
[53] See, for example, T. Shimizu, H. Aoki, H. Yasuoka, T. Tsuda, Y. Ueda, K. Yoshimura, and K. Kosuge, J. Phys. Soc. Jpn. **62**, 3710 (1993).
[54] P. Monthoux and D. Pines, Phys. Rev. B **47**, 6069 (1992).
[55] J. Bardeen, L. N. Cooper, and J. R. Schrieffer, Phys. Rev. **108**, 1175 (1957).
[56] The existence of an effective cutoff energy of about 0.05 eV which is smaller than half of the quasiparticle bandwidth of about 0.2 eV is due to the form factor of the $d\gamma$-wave Cooper pairs.
[57] A. G. Aronov, S. Hikami, and A. I. Larkin, Phys. Rev. Lett. **62**, 965 (1989).
[58] A. A. Abrikosov and L. P. Gorkov, Sov. Phys. JETP **12**, 1243 (1960).
[59] H. Won and K. Maki, Phys. B **49**, 1397 (1994).
[60] The small difference between 4.35 and 4.27 seems to be due to slightly different treatments of the anisotropic dispersion relation of quasiparticles in the two theories.
[61] See, for example, J. R. Kirtley, Int. J. Mod. Phys. B **4**, 201 (1991).
[62] See, for example, S. L. Cooper, M. V. Klein, B. G. Pazol, J. P. Rice, and M. Ginsberg, Phys. Rev. B **37**, 5920 (1988).
[63] See, for example, C. G. Olson, R. Liu, A. B. Yang, D. W. Lynch, A. J. Arko, R. S. List, B. W. Veal, Y. C. Chang, P. Z. Jiang, and A. P. Paulikas, Science **245**, 731 (1989).
[64] See, for example, Z. Schelesinger, R. T. Collins, F. Holtzberg, C. Feild, S. H. Blanton, U. Welp, G. W. Crabtree, Y. Yang, and J. Z. Liu, Phys. Rev. Lett. **65**, 801 (1990).
[65] T. Moriya, Y. Takahashi, and K. Ueda, J. Phys. Soc. Jpn. **59**, 2905 (1990).
[66] See, for example, T. Moriya and K. Ueda, J. Phys. Soc. Jpn. **63**, 1871 (1994). Different notations are used for the phenomenological I by different groups. For example, U_r is used by N. E.

Bickers and S. R. White, Phys. Rev. B **43**, 8044 (1991), $\overline{U}$ by N. Bulut and D. J. Scalapino, Phys. Rev. Lett. **68**, 706 (1992), and $\overline{g}(\mathbf{q})$ by P. Monthoux, A. Balatsky, and D. Pines, Phys. Rev. B **46**, 14 803 (1992).

[67] F. J. Ohkawa, Prog. Theor. Phys. Suppl. **106**, 95 (1991).

[68] F. J. Ohkawa, J. Magn. Magn. Mater. **90 & 91**, 135 (1990).

[69] F. J. Ohkawa, J. Phys. Soc. Jpn. **61**, 627 (1992).

[70] F. J. Ohkawa, J. Phys. Soc. Jpn. **61**, 952 (1992).

[71] F. J. Ohkawa, J. Phys. Soc. Jpn. **61**, 1157 (1992).

[72] K. Maki and H. Won, Phys. Rev. Lett. **72**, 1758 (1994).

[73] L. Krusin-Elbaum, R. L. Greene, F. Holtzberg, A. P. Malozemoff, and Y. Yeshurun, Phys. Rev. Lett. **62**, 217 (1989).

[74] A. T. Fiory, A. F. Hebberd, P. M. Mankiewich, and R. E. Howard, Phys. Rev. Lett. **62**, 1873 (1989).

[75] See, for example, K. Ichimura and K. Nomura, J. Phys. Soc. Jpn. **62**, 3661 (1993).

[76] F. J. Ohkawa, Phys. Rev. B **42**, 371 (1990).

[77] F. J. Ohkawa, Solid State Commun. **76**, 145 (1990).

[78] F. J. Ohkawa, J. Phys. Soc. Jpn. **61**, 635 (1992).

[79] M. Tei, H. Takai, K. Mizoguchi, and K. Kume, Z. Naturforsch. A **45**, 429 (1990).

[80] M. Tei, H. Matsuzawa, H. Sakamoto, K. Mizoguchi, and K. Kume, Physica C **185-189**, 1227 (1991).

[81] K. Kumagai, Y. Nakamichi, Y. Nakamura, T. Takatsuka, and H. Nakajima, J. Phys. Soc. Jpn. **59**, 2336 (1990).

[82] Y. Itoh, H. Yasuoka, and Y. Ueda, J. Phys. Soc. Jpn. **59**, 3463 (1990).

[83] A. Georges and G. Kotliar, Phys. Rev. B **45**, 6470 (1992).